

Supplementary Information

Supplementary Methods

Patient cases from the literature

To identify patients, we searched Pubmed for articles with human subjects written in English using the search terms “(“antisocial” OR “incarcerated” OR “murder” OR “rape” OR “assault” OR “theft” OR “pedophilia” OR “criminal” OR “sociopathy” OR “psychopathy”) AND (“MRI” OR “CT” OR “neuroimaging” OR “lesion”) AND (“damage” OR “stroke” OR “hemorrhage” OR “tumor” OR “lesion”). 221 studies were identified (Supplementary Figure S1. 140 studies were excluded because no crime occurred; 35 studies were excluded because they involved victims of crimes; 4 studies were excluded because no neuroimaging was performed; 21 studies were excluded because they reported group data, but not individual case data; and 5 studies were excluded because no individual patient images were available. An additional 5 studies were found from review of references. A total of 45 cases were identified from studies that met inclusion criteria. 3 cases were excluded because they involved an external, compressive lesion, making lesion tracing difficult, and 2 cases were excluded because poor image quality limited the ability to accurately trace the lesion. Of the remaining 40 cases, 9 (23%) involved murder, 21 (53%) involved other violent crimes, 5 (13%) involved sexual crimes, and 7 (18%) involved nonviolent crimes. 17 had a clear temporal relationship between the lesion and criminal behavior (documented no criminal behavior prior to lesion (15 cases) or resolution of criminal behavior following treatment of lesion (2 cases)) and were included in the high probability group (Table S1). The remaining 23 lesions had an uncertain temporal

association between lesion onset and criminal behavior and were used in a replication cohort (Table S1).

Lesion localization

Published images were used to map each lesion location to a common brain atlas (Figure 1; Supplementary Figure S4). Lesions were traced by hand onto a standardized brain atlas (2x2x2 MNI space) using FSL as in prior work (1–5). All available images were traced for each patient. All cases reported that lesions were focal.

Lesion network mapping

Our group recently developed a technique termed lesion network mapping that identifies brain regions functionally connected to lesion locations causing a given neuropsychiatric symptom (1–7). This technique avoids the need to perform functional brain imaging on the patients themselves and has been validated across many different neurological syndromes. Briefly, traced lesions were used as individual seeds in a resting-state connectivity analysis using data from obtained from 1000 healthy subjects using a 3T Siemens MRI as part of the genome superstructure project (<http://neuroinformatics.harvard.edu/gsp/>). Processing included a temporal filter to remove frequencies above 0.08 Hz; regression of 6 motion parameters, average signal over the entire brain, average signal in the cerebral spinal fluid, and average signal from the white matter; and spatial smoothing at 6 mm FWHM as previously described (8). Functional connectivity to each lesion was determined by calculating the correlated time-course between each lesion location and every other brain voxel using the resting state data from each individual normal control, as described in our prior studies using this connectome (7, 6). These

correlations for all 1000 subjects were then combined to calculate a T-score value for every individual voxel. Both positive and negative correlations with the time course of the lesion location were included. Voxels were thresholded at $T > \pm 12$ in order to create a binarized map of significantly functionally connected regions to each patient's lesion site ($P < 10^{-17}$ uncorrected). A threshold of $t > 12$ was chosen because this resulted in a similar volume and spatial distribution of positively and negatively correlated voxels as a threshold of $t > 4.25$ across a smaller connectome dataset of 98 subjects used in prior lesion network mapping studies (1–5) (Supplementary Figure S6). Finally, maps from each of the patients were combined to form the lesion network mapping overlap for the group, showing the number of patients with lesions functionally connected with each individual voxel (Figure 2C).

Comparison to lesions causing other neurological syndromes

Lesion network mapping results from lesions associated with criminal behavior were compared to lesion network mapping results from lesions causing other syndromes in order to assess specificity. 63 lesions causing auditory hallucinations, visual hallucinations, post-stroke pain, or subcortical aphasia were used as control lesions (1). Voxel-wise nonparametric testing with non-parametric mapping software (<http://www.mccauslandcenter.sc.edu/mricro/npm/>) was used to identify voxels significantly more likely to be connected with lesions causing acquired criminal behavior compared to control lesions using a voxel-wise Lieberman test (9). Voxels affected in <10% of cases were ignored. The resulting Z-maps were thresholded to a standard Bonferroni corrected family-wise error rate of $p < 0.05$ (Figure 3).

Neuroimaging meta-analyses of morality

To define regions involved in morality, we performed an automated meta-analysis of task-fMRI activation studies using the terms “morality”, “value”, “theory of mind”, “empathy”, and “cognitive control” using Neurosynth (www.neurosynth.org), a data-driven, automated engine for performing neuroimaging meta-analyses (10). Briefly, text-mining techniques are used to extract neuroimaging studies using specific terms (at a frequency of >1 in 1,000 words) from a database of 11,406 studies. Next, coordinates from activated regions are automatically extracted from tables in the text using an automated algorithm. Similar to the multilevel kernel density analysis (MDKA) technique, binarized maps are made for each study where a voxel=1 if it occurred within 10mm of a foci reported in the article, or a value of 0 if it did not. Finally, Chi-Square test of independence was used to determine statistical inference maps, corrected for multiple comparisons using a whole brain false-discovery rate (FDR) of 0.05.

The meta-analysis can produce two statistical results: 1.) The probability that studies involving a specific term will show activation in a given region (forward inference), or 2.) The probability that activation in a specific region will be associated with studies using a specific term (reverse inference). Whereas forward inference testing may identify brain regions that are consistently but non-selectively activated in studies involving a specific term, reverse-inference testing will identify regions that, when activated, specifically predict that the study will involve a specific term. We used results from the reverse inference analyses, as the purpose in our study was to identify brain regions specifically associated with the psychological construct of morality.

To ensure that results were not dependent on our choice of meta-analysis technique, we utilized the results of a recent, manually performed meta-analysis of fMRI studies contrasting moral vs. non-moral stimuli (11) using activation likelihood estimation (ALE) (12). Please see

Bzdok et al for full details regarding selection criteria and the ALE method (11). Briefly, a 3D Gaussian probability distribution is created centered on each individual foci and modified by the sample size from each study in order to estimate the spatial uncertainty surrounding each focus. These distributions are then combined across all experiments to arrive at the activation likelihood estimate maps. Finally, a cluster-level inference is used to determine significance. The true convergence on the ALE is compared against a null distribution of 1000 simulated datasets with identical number of foci, experiments, and subjects, but with the foci randomly distributed. It should be noted that implementation errors have been found in the ALE software prior to 2015, which may have resulted in inappropriately liberal statistics (13).

Connectivity of lesions associated with criminal behavior to regions involved in morality

We determined whether lesion locations in patients with criminal behavior showed greater connectivity to regions involved in morality, defined as a binarized map of significant regions identified from each meta-analysis. fMRI time courses were extracted from each lesion location and the binarized map of significant regions from each meta-analysis. The Pearson's correlation coefficient between time courses was computed for each subject in our normative 1000-subject dataset. Resulting r values were converted to a normal distribution using Fischer's r to z transform and statistically compared using a two-tailed t -test. Lesion locations causing acquired criminal behavior were compared to lesion locations causing other neurological syndromes from our previously published work (1). These syndromes included auditory hallucinations, visual hallucinations, post-stroke pain, and subcortical aphasia. All statistics were computed using the statistical package STATA (College Station, TX, version 14.0).

Connectivity to regions involved in specific psychological components of morality

As before, the average Pearson's correlation coefficient was calculated between each lesion location and regions in each of the four meta-analyses. Significance was calculated using a two-tailed t-test, Bonferroni corrected for multiple comparisons (the four meta-analyses) by dividing the p value by 4 ($0.05/4 = 0.0125$).

Connectivity to Regions Involved in Personal and Impersonal Moral Dilemmas

We obtained activation maps for personal moral dilemmas and impersonal moral dilemmas from Greene et al (14). Time-course correlations and statistical comparisons were performed as above. To test if the combination of connectivity to regions activated by personal and impersonal dilemmas was superior to connectivity to either set of regions alone, we performed a likelihood ratio test. Specifically, a logistic regression was performed to predict lesion group (criminality vs. controls) based on a lesion's connectivity to either personal or impersonal regions, compared with the model including connectivity to personal AND impersonal regions.

Connectivity to Regions Involved in the Ultimatum Game

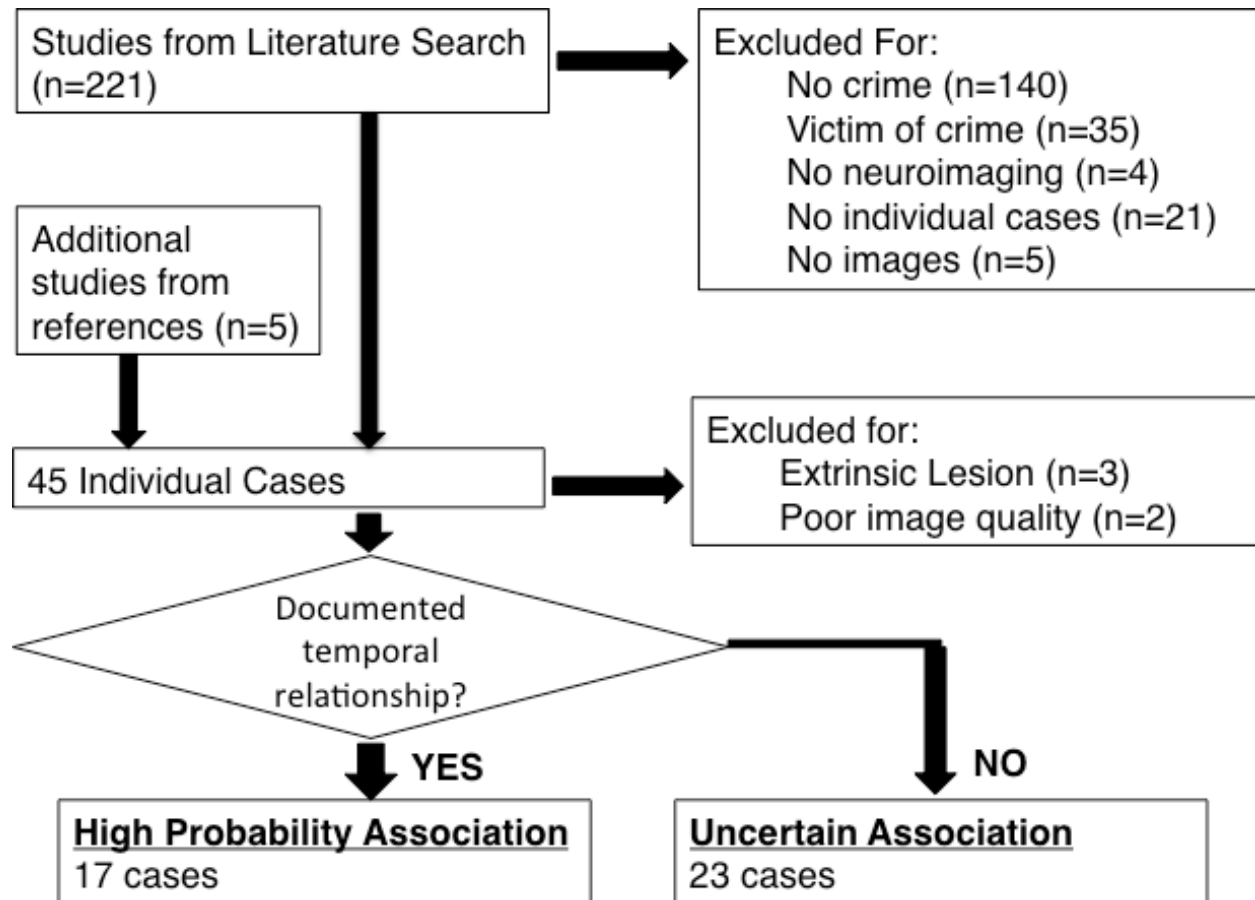
To determine regions of interest for this task, we took advantage of a recently published, coordinate-based ALE meta-analysis of fMRI studies (15). Unfortunately, we were unable to directly obtain the full ALE maps from this analysis. Instead, we created 8mm radius regions of interest (ROI's) at the peak reported coordinates identified for accepting fair offers, and rejecting

unfair offers. We then performed an identical analysis to above in order to statistically test the correlation between lesions locations and the ROI's for fair and unfair offers in the ultimatum game. To demonstrate the validity of this approach, we performed an identical procedure to create ROI's at the peak foci of activation for personal and impersonal moral dilemmas from Greene et al (14), obtaining nearly identical results to those obtained using the full activation maps (Supplementary Figure S7).

Patient factor analyses

First, we explored whether different lesion connectivity patterns might be associated with different types of crimes: 1.) Extremely Violent (murder; n=9), Other Violent (n=21), sexual (rape and pedophilia; n=5, two also involved murder),

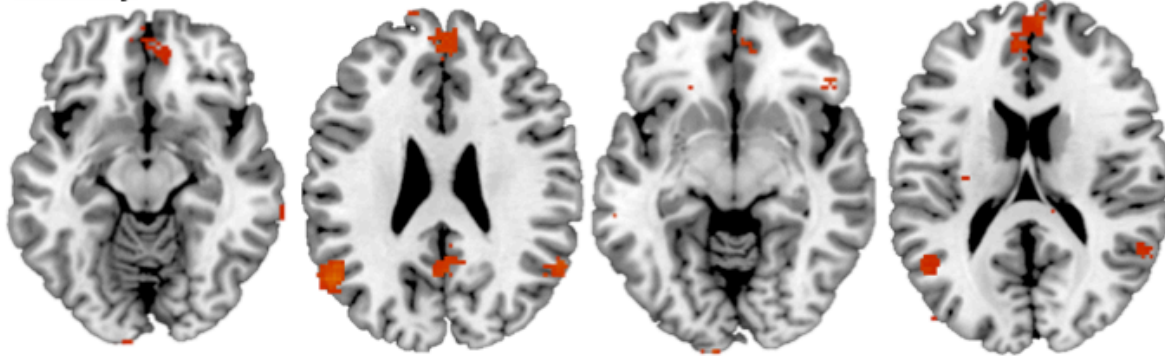
Supplementary Figures S1-S7



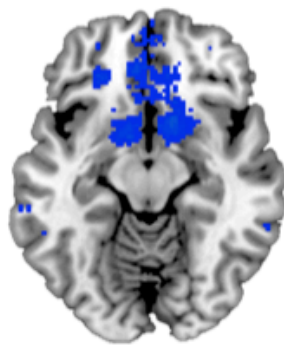
Supplementary Figure S1: Case Selection. Our search identified 221 candidate studies.

Studies were excluded if there was no crime (n=140), involved the victim of a crime (n=35), did not include neuroimaging (n=4), did not describe individual cases (n=21), or did not include neuroimaging images for the patient (n=5). An additional 5 studies were selected from review of references. 45 cases in these studies were identified; 3 were excluded due to external, compressive lesions, and 2 were excluded due to poor image quality. The remaining 40 studies were divided into cases where a clear temporal relationship between the lesion and criminal behavior could be established (n=17) vs. cases without a clear temporal relationship (n=23)

Morality



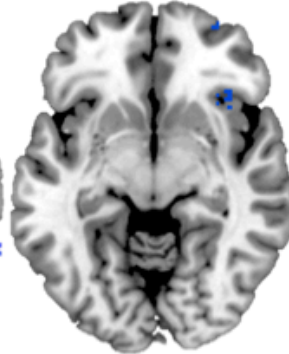
Value



Theory of Mind



Cognitive Control



Empathy

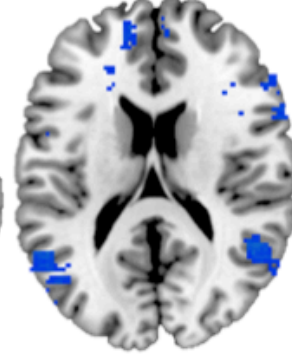
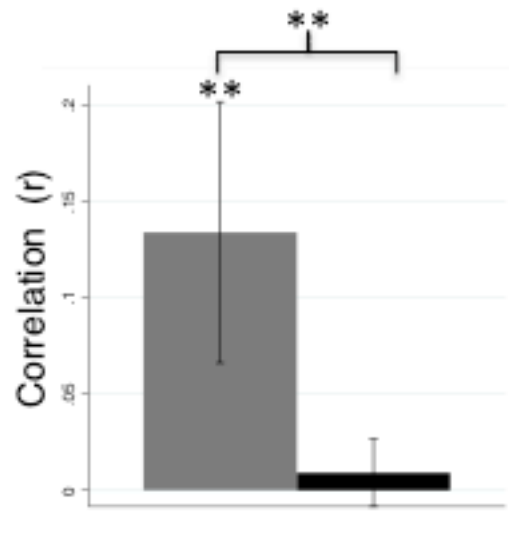
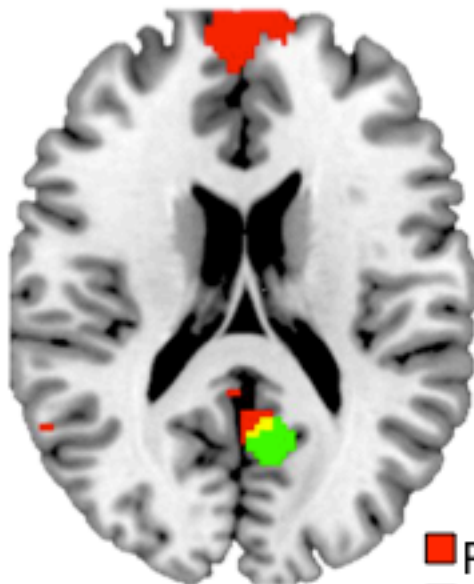
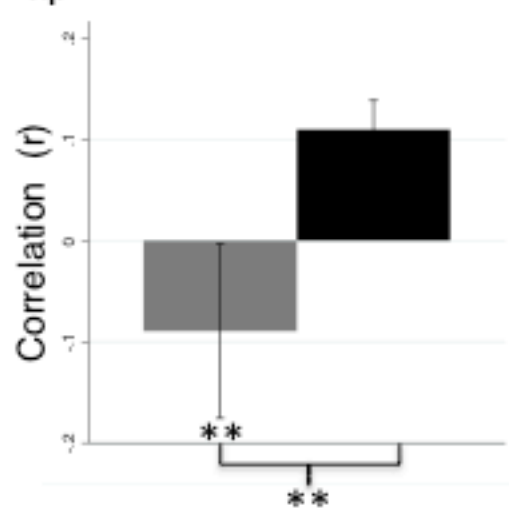
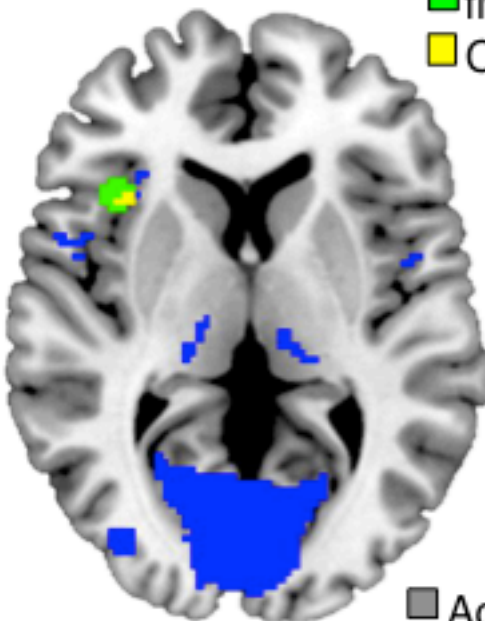


Fig. S2: Neurosynth Meta-analysis regions for Morality Compared to Value, Theory of Mind, Cognitive Control, and Empathy.

A. Accept Offer



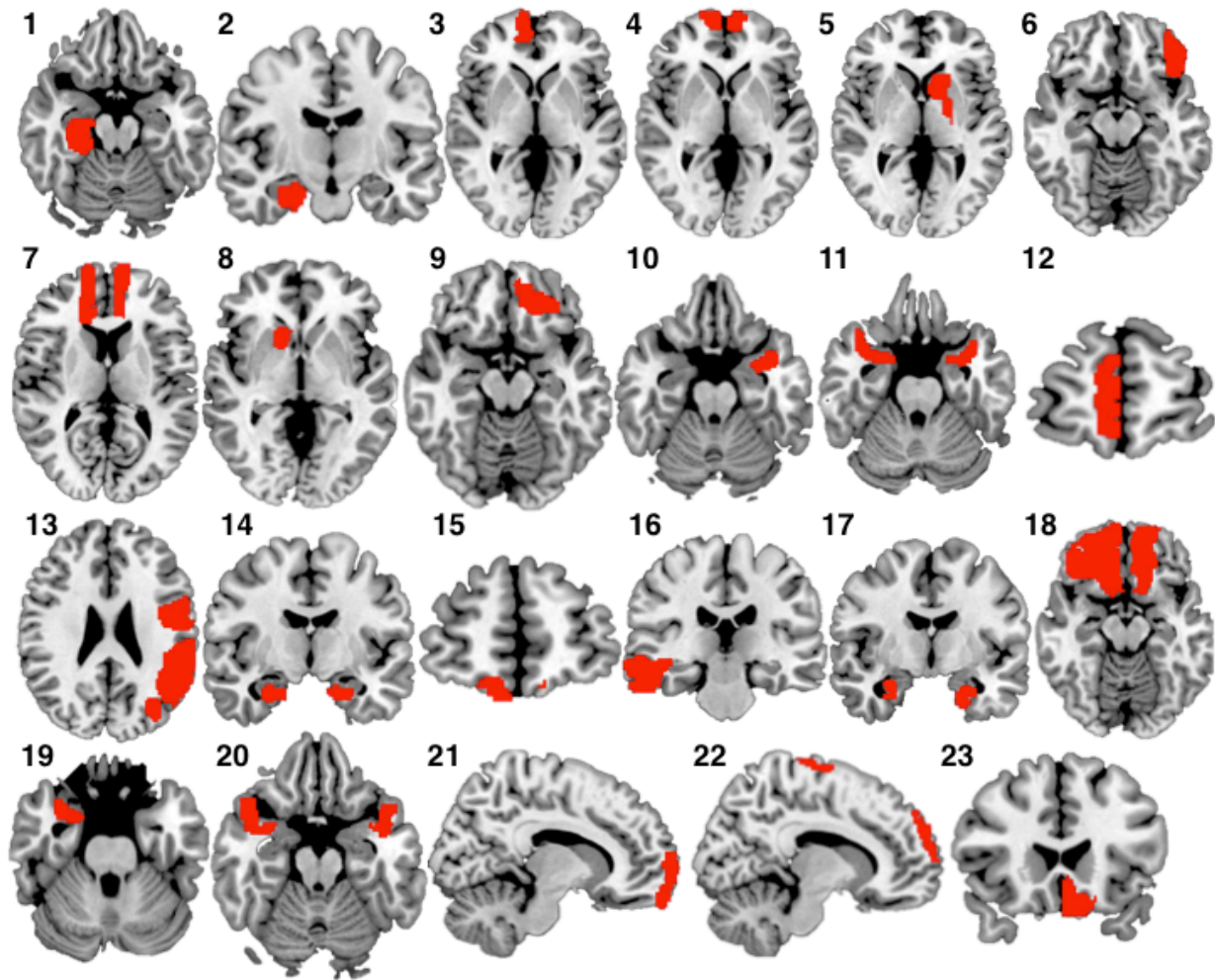
B. Reject Offer



■ Acquired Criminality
■ Control Syndromes

Fig. S3: Connectivity to regions involved in ultimatum game predicts rejection of unfair offers in acquired criminality. On the left, the peak brain region most activated in fair offers,

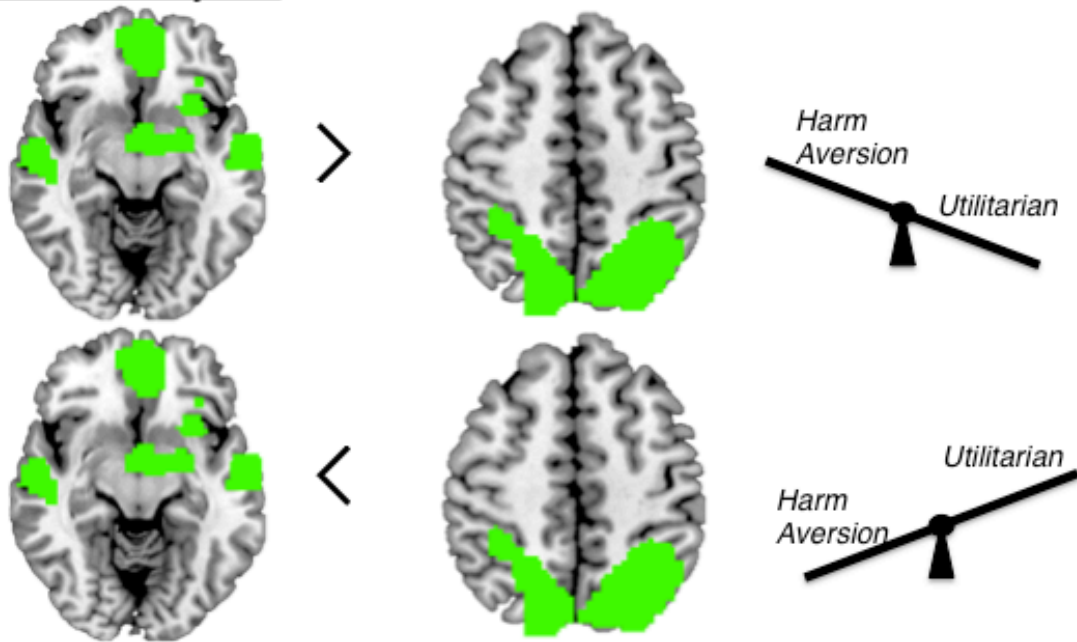
involving decision to accept (**A**) or unfair offers, involving decision to reject (**B**), overlaid on nonparametric statistical maps comparing patients with criminal behavior vs. control lesions (thresholded at $z > 6$) . On the right, the temporal correlation in spontaneous fMRI activity between lesion locations and regions identified in meta-analyses were computed using a cohort of healthy subjects. Correlations were averaged across our 16 lesion locations causing acquired criminal behavior (red) and compared to 77 lesions causing other neurological syndromes (control syndromes, blue). * $p < 0.05$; ** $p < 0.01$, *** $p < 0.001$



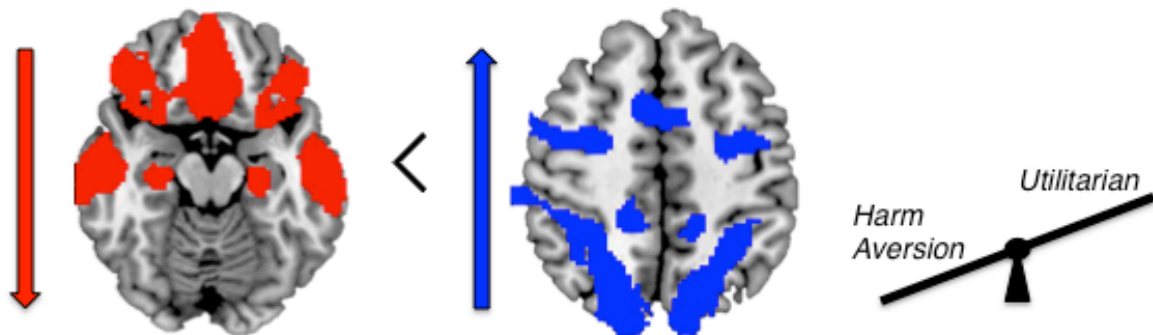
Supplementary Figure S4: Lesions with uncertain association to Criminal Behavior.

Lesions from 23 patients with acquired criminal behavior, manually traced onto a common brain atlas (MNI).

A. Normal Subjects

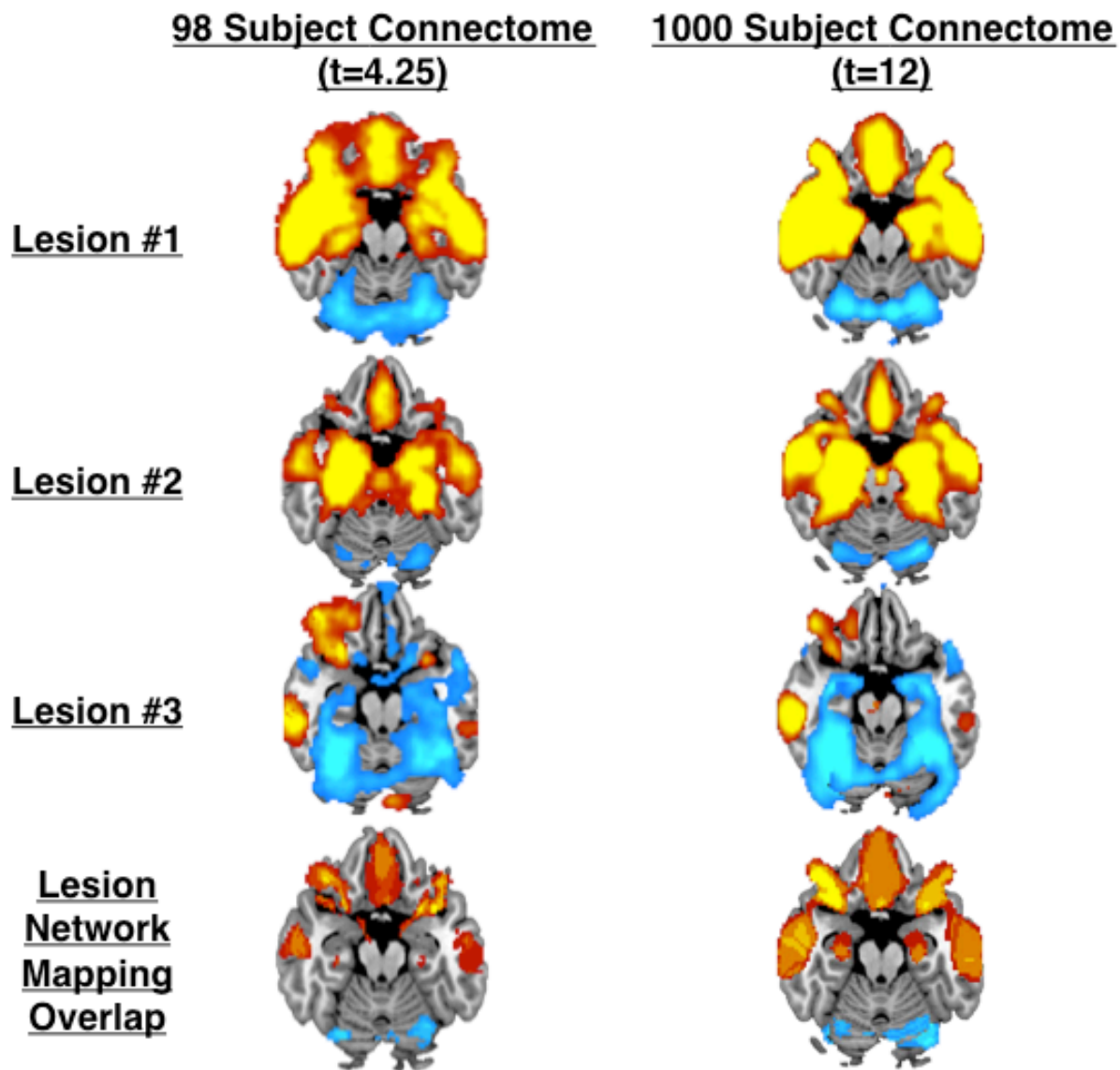


B. Predicted Effects Acquired Criminality Lesions



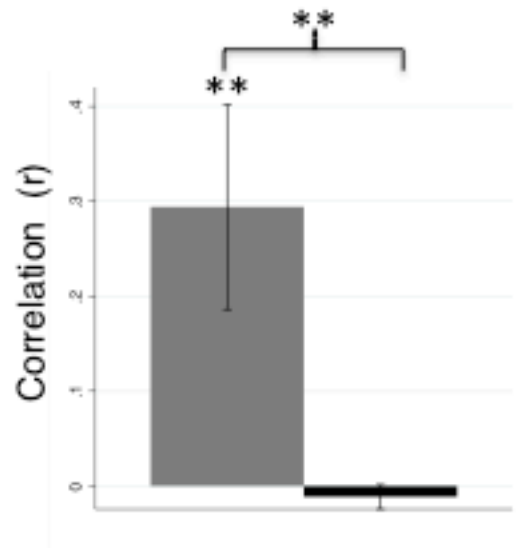
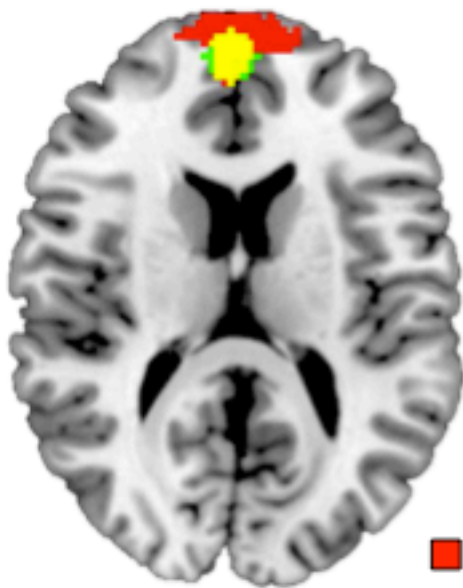
Supplementary Figure S5: Connectivity to regions involved in personal/impersonal moral dilemmas predicts utilitarian choices in acquired criminality.

A) Decisions to avoid harming a person for the greater good are associated with activation in the medial prefrontal cortex (left), while utilitarian decisions are associated with activation in the posterior parietal cortex (right). (B) Based on connectivity, lesions causing criminal behavior should bias patients towards utilitarian decisions (see discussion for further details).

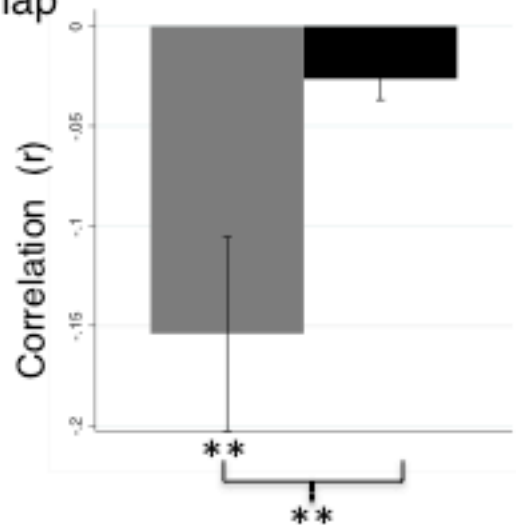
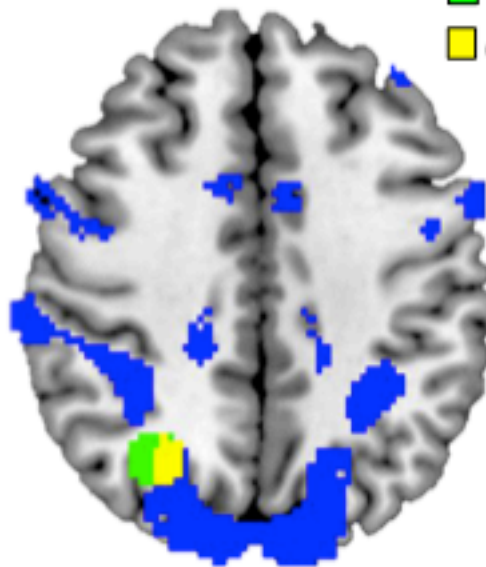


Supplementary Figure S6: Comparison of different cohorts. Lesion network using a 98 subject cohort vs. 1000 subject cohort shows no difference in individual lesions or group level overlap.

A. Personal



B. Impersonal



■ Acquired Criminality
■ Control Syndromes

Fig. S7: Connectivity to regions involved in personal/impersonal moral dilemmas predicts utilitarian choices in acquired criminality. On the left, the peak brain region most activated in personal moral dilemmas, involving decision to avoid harmful action (A) or impersonal moral

dilemmas, involving utilitarian decision **(B)**, overlaid on nonparametric statistical maps comparing patients with criminal behavior vs. control lesions (thresholded at $z > 6$). On the right, the temporal correlation in spontaneous fMRI activity between lesion locations and regions identified in meta-analyses were computed using a cohort of healthy subjects. Correlations were averaged across our 16 lesion locations causing acquired criminal behavior (red) and compared to 77 lesions causing other neurological syndromes (control syndromes, blue). ** $P < 0.0001$

Supplementary Tables S1-S3

Case #	Reference	Behavior	Etiology	Age lesion	Age crime
<i>High Probability Cases</i>					
1	Tonkonogy 1991 (16)	Rage, aggression, arson/fire setting	Abscess resection	16	48
2	Tonkonogy 1991 (16)	Rage, aggression, destruction of property	Trauma	23	42
3	Tonkonogy 1991 (16)	Rage, aggression, destruction of property	Unknown	21	42
4	Anderson 1999 (17)	Verbal/physical aggression, lying, stealing, risky sexual behavior, lack of empathy, guilt, remorse	Trauma	1.5	3
5	Anderson 1999 (17)	Aggression/anger, assault, theft/robbery, lying, risky sexual behavior, lack of empathy, remorse, guilt	Tumor	1	9
6	Meyers 1992 (18)	Lying, risky financial, criminal stealing, fraud	Tumor	33	33
7	Eslinger 1985 (19)	Lying, illegal financial decisions	Tumor	35	35
8	Blair 2000 (20)	Aggression, violence, assault	Trauma	56	56
9	Tranel 2002 (21)	Illegal financial decisions, dishonesty	Stroke	54	54
10	Tranel 2002 (21)	Illegal financial decisions, dishonesty	Sub-arachnoid Hemorrhage	32	32
11	Nakaji 2003 (22)	Aggression, violence, assault, suicide	Tumor	5	14
12	Nakaji 2004 (22)	Violence, aggression	Tumor	4	6
13	Mitchell 2006 (23)	Rape, three separate occasions	Trauma	26	n/a
14	Mitchell 2006 (23)	Murder, rape	Tumor	32	32
15	Mitchell 2006 (23)	Murder, rape on two separate occasions	Trauma	14	18
16	Orellana 2013 (24)	Murder of mother, attempted murder 2 years later	Surgical injury	40	62
17	Sener 2015 (25)	Threat of assault	Trauma	7	34
<i>Uncertain Association</i>					
1	Martinius 1983 (26)	Murder	Unknown		14
2	Muller 2011 (27)	Murder, arson, sadomasochism	Unknown		16
3	Schiltz 2013 (a) (28)	Murder	Unknown		40
4	Schiltz 2013 (b) (28)	Theft	Unknown		22
5	Schiltz 2013 (c) (28)	Aggravated assault	Unknown		61
6	Schiltz 2013 (d, k) (28)	Contract killing	Unknown		49
7	Schiltz 2013 (e, i) (28)	Aggravated assault	Unknown		52
8	Schiltz 2013 (g) (28)	Fraud	Unknown		60
9	Schiltz 2013 (h)	Aggravated assault	Unknown		31

	(28)			
10	Schiltz 2013 (j) (28)	Drug dealing	Unknown	27
11	Schiltz 2013 (j) (28)	Aggravated assault	Unknown	45
12	Trebuchon 2013 (29)	Violence, drug abuse	Cortical dysplasia	0
13	Villano 2009 (30)	Murder	Tumor	55
14	Witzel 2016 (a) (31)	Aggravated assault, robbery	Unknown	25
15	Witzel 2016 (b) (31)	Arson	Unknown	62
16	Witzel 2016 (c) (31)	Manslaughter	Unknown	77
17	Witzel 2016 (d) (31)	Assault	Unknown	57
18	Witzel 2016 (e) (31)	Arson	Unknown	38
19	Witzel 2016 (f) (31)	Sexual child abuse / pedophilia	Unknown	34
20	Witzel 2016 (g) (31)	Murder	Unknown	38
21	Witzel 2016 (h) (31)	Attempted manslaughter	Unknown	43
22	Witzel 2016 (i) (31)	Sexual Assault	Unknown	22
23	Boes 2011 (32)	Violence, aggression, stealing, lying	Heterotopia	0

Table S1: Cases of Acquired Criminal Behavior. Crimes, lesion etiology, and age onset for cases with a documented temporal association between lesion and criminal behavior (high probability, 17 cases) or uncertain association between lesion and criminal behavior (23 cases).

Voxels	Overlap	X	Y	Z	Anatomy (Harvard-Oxford Atlas)
<i>Positive Correlations</i>					
1934	17	2	64	6	frontal pole
1075	17	54	2	-38	anterior inferior / middle frontal gyrus, temporal pole
426	17	38	22	-22	orbital frontal, temporal pole
329	17	-30	16	-18	orbital frontal
38	15	-58	-24	-26	inferior temporal gyrus
34	15	-46	12	-46	anterior temporal pole
26	16	8	4	-2	caudate / nucleus accumbens
24	16	-6	8	-2	caudate / nucleus accumbens
21	16	2	16	-22	subcallosal cortex
<i>Negative Correlations</i>					
6716	17	26	-78	-18	occipital, intraparietal sulcus
129	16	-24	-2	52	superior / middle frontal gyrus
51	15	32	-8	52	superior / middle frontal gyrus
17	16	30	-34	-50	cerebellum
10	15	30	-82	20	lateral occipital

Table S2: Lesion Network Mapping Coordinates. Peak coordinates (MNI space) for all regions that shared connectivity with at least 15 of 17 lesions in patients with clear temporal association between lesion and criminal behavior, minimum of 10 voxels.

Voxels	T score	X	Y	Z	Anatomy (Harvard-Oxford Atlas)
<i>Positive Correlations</i>					
3867	8.7	4	66	8	frontal pole / ventromedial prefrontal cortex
2770	8.7	54	2	-38	temporal pole, anterior inferior / middle temporal gyrus, orbital frontal cortex
2037	8.08	-30	18	-18	orbital frontal cortex
39	7.38	-46	-68	40	lateral occipital cortex / angular gyrus
25	7.38	0	-52	24	posterior cingulate cortex
18	7.38	24	-14	-20	hippocampus
14	7.38	54	-60	30	lateral occipital cortex / angular gyrus
12	7.38	-28	-14	-16	hippocampus / amygdala
10	7.38	-50	-68	24	lateral occipital cortex / angular gyrus
<i>Negative Correlations</i>					
3075	8.7	-12	-76	-16	lingual / occipital, intraparietal sulcus
590	8.21	-4	-56	64	intraparietal sulcus
208	7.38	-6	8	42	anterior cingulate cortex
189	8.21	-24	-2	52	superior / middle frontal gyrus
179	7.78	26	0	56	dorsolateral prefrontal cortex
118	8.7	-30	-58	48	intraparietal sulcus
65	7.12	22	-72	34	lateral occipital cortex
64	8.21	30	-34	-50	cerebellum
27	7.78	64	10	34	precentral gyrus
26	7.78	-60	10	32	precentral gyrus
22	7.78	-32	-36	-50	cerebellum
21	7.38	38	-42	40	intraparietal sulcus
19	7.38	-26	-72	-56	cerebellum

Table S3: Voxel-Based Lesion Network Symptom Mapping Coordinates. Peak coordinates (MNI space) for all regions that showed significantly greater connectivity in patients with clear temporal association between lesion and criminal behavior, compared to control lesions, threshold at $t > 7$, minimum of 10 voxels.

Supplementary References

1. Boes AD, et al. (2015) Network localization of neurological symptoms from focal brain lesions. *Brain* 138(10):3061–3075.
2. Darby RR, Laganier S, Pascual-Leone A, Prasad S, Fox MD (2017) Finding the imposter: brain connectivity of lesions causing delusional misidentifications. *Brain* 140(2):497–507.
3. Fischer DB, et al. (2016) A human brain network derived from coma-causing brainstem lesions. *Neurology* 87(23):2427–2434.
4. Laganier S, Boes AD, Fox MD (2016) Network localization of hemichorea-hemiballismus. *Neurology* 86(23):2187–2195.
5. Fasano A, Laganier SE, Lam S, Fox MD (2017) Lesions causing freezing of gait localize to a cerebellar functional network. *Ann Neurol* 81(1):129–141.
6. Darby RR, Fox MD (2017) Reply: Capgras syndrome: neuroanatomical assessment of brain MRI findings in an adolescent patient. *Brain* 140(7):e44.
7. Horn A, et al. (2017) Connectivity predicts deep brain stimulation outcome in Parkinson's disease. *Ann Neurol*:1–39.
8. Thomas Yeo BT, et al. (2011) The organization of the human cerebral cortex estimated by intrinsic functional connectivity. *J Neurophysiol* 106(3):1125–1165.
9. Rorden C, Karnath H-O, Bonilha L (2007) Improving lesion-symptom mapping. *J Cogn Neurosci* 19(7):1081–8.
10. Yarkoni T, Poldrack RA, Nichols TE, Van Essen DC, Wager TD (2011) Large-scale automated synthesis of human functional neuroimaging data. *Nat Methods* 8(8):665–670.
11. Bzdok D, et al. (2012) Parsing the neural correlates of moral cognition: ALE meta-analysis on morality, theory of mind, and empathy. *Brain Struct Funct* 217(4):783–96.
12. Eickhoff SB, et al. (2009) Coordinate-based activation likelihood estimation meta-analysis of neuroimaging data: a random-effects approach based on empirical estimates of spatial uncertainty. *Hum Brain Mapp* 30(9):2907–26.
13. Eickhoff SB, Laird AR, Fox PM, Lancaster JL, Fox PT (2017) Implementation errors in the GingerALE Software: Description and recommendations. *Hum Brain Mapp* 38(1):7–11.
14. Greene JD, Nystrom LE, Engell AD, Darley JM, Cohen JD (2004) The neural bases of cognitive conflict and control in moral judgment. *Neuron* 44(2):389–400.
15. Feng C, Luo Y-J, Krueger F (2015) Neural signatures of fairness-related normative

- decision making in the ultimatum game: a coordinate-based meta-analysis. *Hum Brain Mapp* 36(2):591–602.
16. Tonkonogy JM (1991) Violence and temporal lobe lesion: head CT and MRI data. *J Neuropsychiatry Clin Neurosci* 3(2):189–196.
 17. Anderson SW, Bechara A, Damasio H, Tranel D, Damasio AR (1999) Impairment of social and moral behavior related to early damage in human prefrontal cortex. *Nat Neurosci* 2(11):1032–7.
 18. Meyers CA, Berman SA, Scheibel RS, Hayman A (1992) Case report: acquired antisocial personality disorder associated with unilateral left orbital frontal lobe damage. *J Psychiatry Neurosci* 17(3):121–5.
 19. Eslinger PJ, Damasio a R (1985) Severe disturbance of higher cognition after bilateral frontal lobe ablation: patient EVR. *Neurology* 35(December 1965):1731–1741.
 20. Blair RJR (2000) Impaired social response reversal: A case of ‘acquired sociopathy’. *Brain* 123(6):1122–1141.
 21. Tranel D, Bechara A, Denburg NL (2002) Asymmetric functional roles of right and left ventromedial prefrontal cortices in social conduct, decision-making, and emotional processing. *Cortex* 38(4):589–612.
 22. Nakaji P, Meltzer HS, Singel SA, Alksne JF (2003) Improvement of aggressive and antisocial behavior after resection of temporal lobe tumors. *Pediatrics* 112(5):e430.
 23. Mitchell DG V, et al. (2006) Instrumental learning and relearning in individuals with psychopathy and in patients with lesions involving the amygdala or orbitofrontal cortex. *Neuropsychology* 20(3):280–289.
 24. Orellana G, et al. (2013) Psychosis-related matricide associated with a lesion of the ventromedial prefrontal cortex. *J Am Acad Psychiatry Law* 41(3):401–6.
 25. Sener MT, Ozcan H, Sahingoz S, Ogul H (2015) Criminal Responsibility of the Frontal Lobe Syndrome. *Eurasian J Med* 47(3):218–22.
 26. Martinus J (1983) Homicide of an aggressive adolescent boy with right temporal lesion: a case report. *Neurosci Biobehav Rev* 7(3):419–22.
 27. Müller JL (2011) Are sadomasochism and hypersexuality in autism linked to amygdalohippocampal lesion? *J Sex Med* 8(11):3241–9.
 28. Schiltz K, Witzel JG, Bausch-Hölterhoff J, Bogerts B (2013) High prevalence of brain pathology in violent prisoners: a qualitative CT and MRI scan study. *Eur Arch Psychiatry Clin Neurosci* 263(7):607–16.
 29. Trebuchon A, Bartolomei F, McGonigal A, Laguitton V, Chauvel P (2013) Epilepsy & Behavior Reversible antisocial behavior in ventromedial prefrontal lobe epilepsy. *Epilepsy Behav* 29(2):367–373.
 30. Villano JL, Mlinarevich N, Watson KS, Engelhard HH, Anderson-Shaw L (2009) Aggression in a patient with primary brain tumor: ethical implications for best management. *J Neurooncol* 94(2):293–6.
 31. Witzel JG, Bogerts B, Schiltz K (2016) Increased frequency of brain pathology in inmates of a high - security forensic institution : a qualitative CT and MRI scan study. *Eur Arch Psychiatry Clin Neurosci* 266(6):533–541.
 32. Boes AD, et al. (2011) Behavioral effects of congenital ventromedial prefrontal cortex malformation. *BMC Neurol* 11(1):151.